Articles

Scanning Tunneling Microscopy Observation of Sulfur Electrodeposits on Graphite Single Crystals[†]

J. L. Zubimendi, R. C. Salvarezza, L. Vázquez,[‡] and A. J. Arvia*

*Instituto de Investigaciones Fisicoquímicas Teóricas y Aplicadas, Sucursal 4,
Casilla de Correo 16, (1900) La Plata, Argentina*

The early stages of sulfur deposit growth on highly oriented pyrolytic graphite (HOPG) caused by HS^- electrooxidation in a neutral buffered solution have been investigated using electrochemical techniques and ex situ scanning tunneling microscopy (STM). In this system sulfur deposition has been observed at -0.80 V vs SCE, i.e. a potential more negative than the reversible potential for the HS^-/S reaction. The charge density was equivalent to an average surface coverage by sulfur atoms $\theta \cong 1/3$ monolayer (ML). Ex situ atomic resolution STM images of the layer electrodeposited at -0.8 V show sulfur submonolayers and large uncovered HOPG domains. Sulfur electroadsorption layers appear as a diluted $(\sqrt{3}\times\sqrt{3})$ surface phase with S atoms atop C atoms of the graphite hexagons and the S$-$S interatomic distance $d(S-S) = 0.42$ nm. Further addition of S atoms to a diluted sulfur phase resulted in the formation of sulfur trimers with three S atoms placed atop the three C atoms constituting the graphite hexagons. In this case $d(S-S) = 0.24$ nm. Neighbor trimers originate a filled hexagonal lattice. Ex situ STM images of overpotential deposited sulfur also show submonolayer sulfur domains with a second hexagonal $(\sqrt{3}\times\sqrt{3})R30°$ sulfur lattice with $d(S-S) = 0.42$ nm. A further increase of θ produces either a new honeycomb lattice with $d(S-S) = 0.24$ nm or a rectangular lattice formed by rows of S atoms with $d(S-S) = 0.21$ nm and row separation $d(S-S) = 0.37$ nm.

1. Introduction

The chemisorption of sulfur has been extensively investigated on body-centered cubic (bcc) and face-centered cubic (fcc) metal surfaces using low-energy electron diffraction (LEED) and scanning tunneling microscopy (STM) under ultrahigh vacuum (UHV) conditions.[1−5]

It has been reported that at low surface coverages, adsorbed sulfur formed $c(2\times2)$ open lattices on (100) surfaces of bcc and fcc metals, and $(\sqrt{3}\times\sqrt{3})R30°$ structures on the (111) and (0001) surfaces of fcc and hcp metals.[1,6,7] Furthermore, different types of S atom lattices were observed by STM in UHV, depending on both the substrate nature and the degree of surface coverage by S atoms, the S$-$metal substrate binding changing with surface coverage.[4] However, due to the high stability of sulfur layers in the atmosphere, atomic resolution of these layers on Pt(100) has also been obtained in air.[8]

The presence of S-containing adsorbed species becomes particularly relevant for a number of electrochemical systems, as this type of adsorbate considerably modifies the stability of metals in different environments and also behaves as poisons of several electrocatalytic reactions.[1] Electrochemical,[1,9] X-ray photoelectron spectroscopy (XPS),[9] electroreflectance,[10] and Raman spectroscopy[11] data on sulfur electroadsorption on various metals from aqueous solutions have been reported. The sulfur electrodeposition goes from the underpotential deposition of submonolayers to the overpotential formation of sulfur or polysulfide multilayers.

Recently, the surface structure of sulfur layers produced on Au(111) in the overpotential range from Na_2S-containing perchlorate acid solution has been studied by in situ STM.[12] In this case, the $(\sqrt{3}\times\sqrt{3})R30°$ lattice structure previously reported in vacuum for different sulfur/metal systems has also been observed.[3,4] This layer was assigned to monomeric sulfur S on Au(111) substrate. Besides, square patterns with values of $d(S-S)$, the S$-$S interatomic distance, greater than that in bulk sulfur phase were determined. These square patterns were interpreted as S_8-rings atop the $(\sqrt{3}\times\sqrt{3})R30°$ layer. These results were compared to those resulting from Au(111) surfaces after being exposed to oxygen-containing solutions in the presence of S^{2-}, SCN^-, and *n*-octadecanethiol.[13,14] In these cases, square patterns with $d = 0.27$ nm were observed, irrespective of the S-containing molecule. From these data

---

[†] Presented at the symposium on Advances in the Measurement and Modeling of Surface Phenomena, San Luis, Argentina, August 24−30, 1994.

[‡] Visiting Professor from Instituto de Ciencia de Materiales, CSIC, C-XII, Universidad Autónoma de Madrid, 28049 Madrid, Spain.

[⊗] Abstract published in *Advance ACS Abstracts,* January 1, 1996.

(1) Bénard, J., Ed. *Adsorption on Metal Surfaces*; Elsevier: New York, 1983, and references therein.

(2) Hwang, R. Q.; Zeglinski, D. M.; Lopez Vazquez-de-Parga, A.; Ogletree, D. F.; Somorjai, G. A.; Salmeron, M. *Phys. Rev. B* **1991**, *44*, 1914.

(3) Ogletree, D. F.; Ocal, C.; Marchon, B.; Somorjai, G. A.; Salmeron, M.; Beebe, T. P.; Siekhaus, W. *J. Vac. Sci. Technol. A* **1990**, *8*, 297.

(4) Ogletree, D. F.; Hwang, R. Q.; Zeglinski, D. M.; Lopez Vazquez-de-Parga, A.; Somorjai, G. A.; Salmeron, M. *J. Vac. Sci. Technol. B* **1991**, *9*, 886.

(5) Widring, C. A.; Alves, C. A.; Porter, M. D. *J. Am. Chem. Soc.* **1991**, *113*, 2805.

(6) Othani, H.; Kao, C. T.; Van Hove, M. A.; Somorjai, G. A. *Prog. Surf. Sci.* **1986**, *23*, 155.

(7) Van Hove, M. A.; Wang, S. W.; Ogletree, D. F.; Somorjai, G. A. *Quantum Chem.* **1989**, *20*, 1.

(8) Maurice, V.; Marcus, P. *Surf. Sci.* **1992**, *262*, L 59.

(9) Buckley, A. N.; Halminton, I. C.; Woods, R. *J. Electroanal. Chem.* **1987**, *216*, 213.

(10) Lezna, R. O.; Tacconi, N.; Arvia, A. J. *J. Electroanal. Chem.* **1990**, *283*, 319.

(11) Gao, X.; Zhang, Y.; Weaver, M. J. *Langmuir* **1992**, *8*, 668.

(12) Gao, X.; Zhang, Y.; Weaver, M. J. *J. Phys. Chem.* **1992**, *96*, 4156.

(13) McCarley, R. L.; Kim, Y. T.; Bard, A. J. *J. Phys. Chem.* **1993**, *93*, 211, and references therein.

(14) Kim, Y. T.; McCarley, R. L.; Bard, A. J. *J. Phys. Chem.* **1992**, *96*, 7416.
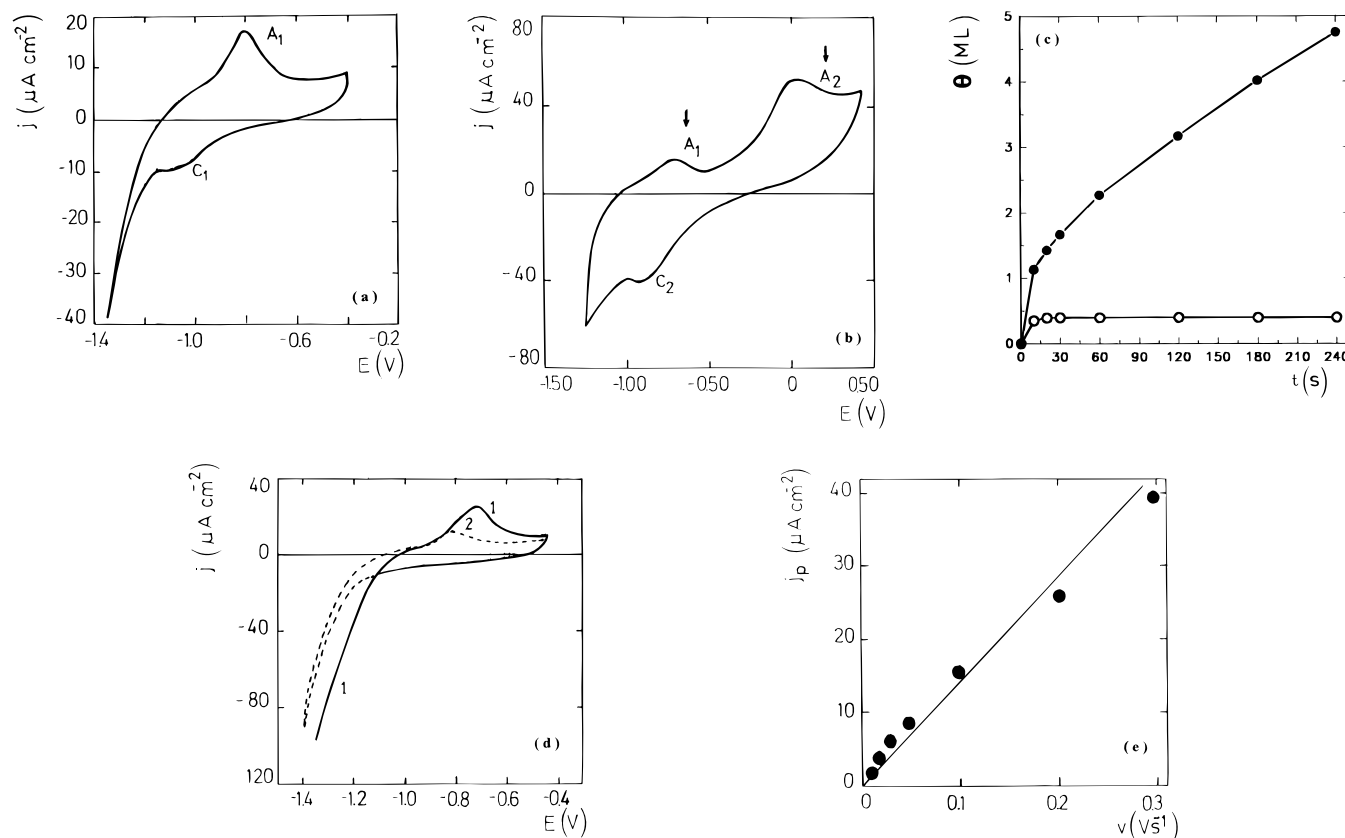

Figure 1. (a) Voltammogram (first scan) for HOPG recorded at 0.1 V/s between -1.4 and -0.4 V in 10^{-3} M Na_2S + borate−boric acid buffer. (b) Voltammogram (first scan) for HOPG recorded at 0.1 V/s between -1.4 and 0.3 V in 10^{-3} M Na_2S + borate−boric acid buffer. (c) θ vs t plots resulting from $E = -0.65$ V (●) and $E = 0$ V (○) in 10^{-3} M Na_2S + borate−boric acid buffer. (d) First and second scans for HOPG recorded at 0.1 V/s between -1.4 and -0.4 V in 10^{-3} M Na_2S + borate−boric acid buffer. (e) Peak current (j) vs sweep rate (v) plots for peak A_1.

it was concluded that these square patterns corresponded to Au atoms on reconstructed Au(111) surfaces produced by Au dissolution. Therefore, these results have left the question about the origin of the surface patterns observed during STM imaging of sulfur layers open to further investigation.

This work refers to the electroformation of sulfur layers on highly oriented pyrolytic graphite (HOPG) by applying ex situ STM complemented with electrochemical measurements. Despite the fact that HOPG is widely used as a well-defined surface for STM imaging, no data on sulfur electrodeposition on this substrate have been found. The ex situ technique was preferred because of the low reactivity of HOPG and S layers in air[8,13] and the avoidance of artifacts which can be due to the electric field created by the tip itself, as reported for in situ Pb electrodeposition on HOPG.[15]

These results show that sulfur deposition on HOPG occurs at a potential more negative than the reversible potential for the SH⁻/S redox reaction and it involves a surface coverage by S atoms close to $^1/_3$. The ex situ STM images reveal a discontinuous sulfur layer with sulfur submonolayers and large uncovered HOPG domains. The sulfur submonolayer domains exhibit either a diluted ($\sqrt{3}\times\sqrt{3}$) surface structure or sulfur trimers. Discontinuous sulfur electrodeposits have also been observed by ex situ STM for deposits grown in the overpotential range. In this case, sulfur-covered domains exhibit a number of distinguishable structures depending on the degree of surface coverage by S atoms.

(15) Hendricks, S. A.; Kim, Y. Z.; Bard, A. J. *J. Electrochem. Soc.* **1992**, *139*, 2818.

2. Experimental Section

Sulfur electrodeposition on HOPG from a 10^{-3} M Na_2S + 0.05 M H_3BO_3 + 0.1 M $Na_2B_4O_7$ (pH 8.0) solution was studied by combining conventional electrochemical techniques with ex situ STM and XPS. The solution chosen for this work was similar to that used in a number of electrochemical, XPS, and electroreflectance spectroscopy studies about sulfur layer formation on metals.[9,10] This choice favored a reliable comparison of results from other sources.

Current density (j) vs potential (E) voltammetric characteristics of sulfur electroformation on HOPG were determined with a conventional electrochemical glass cell consisting of a HOPG working electrode, a Pt polycrystalline counterelectrode, and a saturated calomel reference electrode (SCE). Potentials in the text are given in the SCE scale. Each voltammogram was run with a freshly cleaved HOPG surface immersed in the working solution at 0.1 V s⁻¹ between -1.4 and 0.3 V.

The base buffer was prepared from a.r. reagents and Milli-Q water, deaerated by bubbling, and kept under purified N_2 prior to the electrochemical runs. The sodium sulfide containing solution was made by adding $Na_2S \cdot 9H_2O$ to the deoxygenated borate−boric acid buffer. Electrochemical runs were performed under N_2 at 25 °C.

Sulfur electrodeposition was made at a constant potential set in the -0.65 V $\leq E_d \leq 0.20$ V range for $t = 10$ s electrodeposition time. The sulfur electrodeposit charge density covered the $0.05 < q_d < 0.50$ mC cm⁻² range. After sulfur electrodeposition, the working electrode was removed from the electrochemical cell, carefully rinsed with deoxygenated water, and then dried under N_2 at room temperature. Immediately afterward it was placed into the sample holder of a McAllister STM operating in the atmosphere.

Ex situ STM images were obtained within a short time range and continued for no later than 6 h after sample removal from the cell. Tips used for STM imaging were made by cutting 0.11 mm diameter Pt−Ir wires. STM images were obtained by
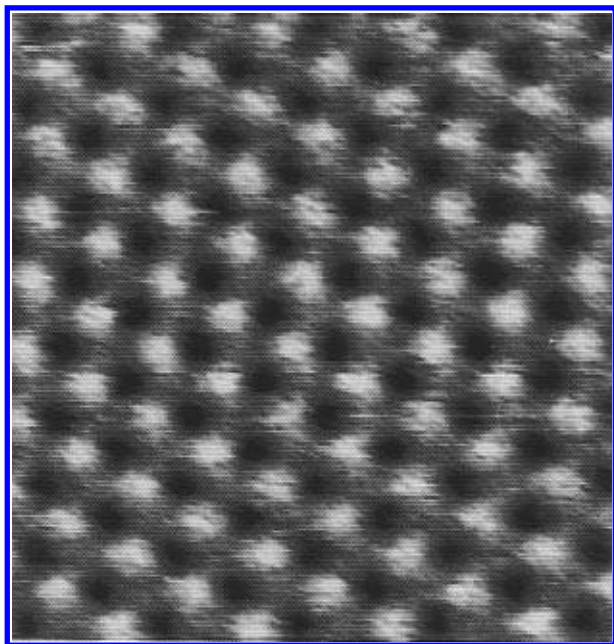
Figure 2. STM image (1.7×1.7 nm^2 top view; $V_t = 2$ mV; $i_t = 5$ nA) of HOPG after polarization at $E = 0.15$ V for $t = 10$ s in the borate buffer. Note that the honeycomb structure is clearly resolved.

applying a 1–90 mV bias voltage with the tip positive at 0.5–5 nA constant current. Atomic distances were measured along the x-axis where the atomic corrugation is faster imaged at ca. 0.05 s scan^{-1}. The topographic and constant-height modes were used for atomic resolution imaging.

Attempts to determine the surface roughness factor of the HOPG electrodes by capacity measurements were made. C_s, the capacity of the HOPG electrode (1 cm^2 geometric area), was estimated by recording voltammograms at different v, the sweep rate (0.01 V s$^{-1} \leq v \leq 0.30$ V s^{-1}), between −1.0 V and 0.3 V in the borate buffer. Under these conditions only I, the current associated to the double layer charging process of the HOPG electrode, was observed as no electrooxidation of the HOPG surface occurs in this potential region.[16] Then, from the slope of the I vs v plots C_s, the specific capacity, results, $C_s = 12$ μF cm^{-2}. This value is close to that already reported for cleaved HOPG[17] although other C_s values are reported for graphite samples with different origin and surface preparation.[18] Therefore, it is not possible to estimate unambiguously the surface roughness factor from capacity measurements. However, visual and optical microscopic examinations of the HOPG surface show a mirror-like appearance. STM images reveal flat areas which extend over several micrometers. Typically, for a 700×700 nm^2 area, total height differences in the order of 1–2 nm and root mean square roughness around 0.1 nm were routinely measured. From these results the surface roughness factor of the HOPG surface was taken equal to 1.

STM calibration was performed by imaging the HOPG surface. At the highest resolution (40×40 nm^2) the typical hexagonal array of C atoms, where only three out of the six C atoms are imaged leading to the nearest neighbors distance $d = 0.24 \pm 0.02$ nm, was observed.[19] However, the honeycomb structure of HOPG with $d = 0.14$ nm was also repeatedly imaged.[19] Data were acquired at a fully automated workstation and stored as digitized images with 200×200 pixels. The scan rate was 300 nm s^{-1}. STM images are presented as raw data. The atomic distances given in this work have been exclusively obtained from raw data images.

(16) Zubimendi, J. L.; Vázquez, L.; Ocón, P.; Vara, J. M.; Triaca, W.; Salvarezza, R. C.; Arvia, A. J. *J. Phys. Chem.* **1993**, *97*, 5095.
(17) Bauer, H. H.; Spritzer, M. S.; Elving, P. J. *J. Electroanal. Chem.* **1968**, *17*, 299.
(18) *Encyclopedia of Electrochemistry of the Elements*; Bard, A. J., Ed.; Marcel Dekker: New York, 1976; Vol. VII.
(19) Binning, G.; Fuchs, H.; Gerber, Ch.; Rohrer, H.; Stoll, E.; Tossati, E. *Europhys. Lett.* **1986**, *1*, 31.
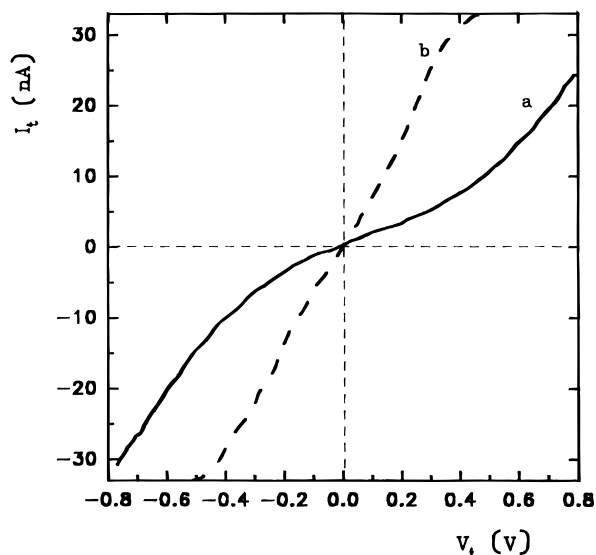

Figure 3. (a) Typical i_t vs V_t plot recorded on HOPG after polarization at $E = 0.15$ V for $t = 10$ s in the borate bufffer. (b) i_t vs V_t plot resulting from a S covered domain.

XPS spectra of S-covered HOPG electrodes were run in Vacuum Generator Scientific ESCA III equipment. The photon energy was Mg Kα 1253.6 eV with the detector at 60° and a collection time between 20 and 60 s.

3. Results and Interpretation

3.1. Electrochemical Data. The first voltammogram recorded at 0.10 V s^{-1} from −1.4 to −0.4 V for HOPG in the Na$_2$S-containing buffer (Figure 1a) shows a relatively broad and small anodic current peak in the −0.80 to −0.70 V range (peak A$_1$). The reverse scan exhibits a poorly defined cathodic current peak (C$_1$) at −1.05 V overlapping the hydrogen evolution reaction (HER) current. By extention of the anodic potential limit to 0.3 V, another broad anodic current peak (peak A$_2$) is observed at about 0.1 V (Figure 1b), and the reverse scan shows a broad cathodic current peak at −0.9 V (peak C$_2$) which completely masks peak C$_1$. The peak A$_1$/peak C$_1$ voltammetric charge ratio is near 1.2 and q_d, the anodic charge density involved in peak A$_1$, is 0.048 ± 0.005 mC cm^{-2}.

The shape and the location of voltammetric peaks resemble those already known for electrochemical reactions involving sulfide/sulfur species on different metals in acid, neutral, or slightly alkaline solutions,[9−11,20] although these reactions appear more irreversible on HOPG. It means that the graphite electrode behaves as a metal for the sulfide electrooxidation. In fact, it has been reported that sulfide oxidation on graphite, nickel, gold, and platinum electrodes in alkaline solutions leads to sulfur or polysulfides species at relatively negative potential values.[21] A common pathway involving the transfer of a sulfur atom from an adsorbed polysulfide ion at the electrode to a polysulfide ion in solution[22] independent of the nature of the inert electrode has been proposed.[21] The formation of an intercalation compound between the HOPG and sulfide ions could also be possible. Intercalation compound formation between graphite and a number of different anions has been reported.[18] However, none has been described for the HOPG/sulfide system. It should be noted that the formation of these compounds requires the electrooxidation of the graphite

(20) Bohé, A.; Vilche, J.; Arvia, A. J. *Corros. Sci.*, in press.
(21) Allen, P. B.; Hickling, A. *Trans. Faraday Soc.* **1957**, *53*, 1626.
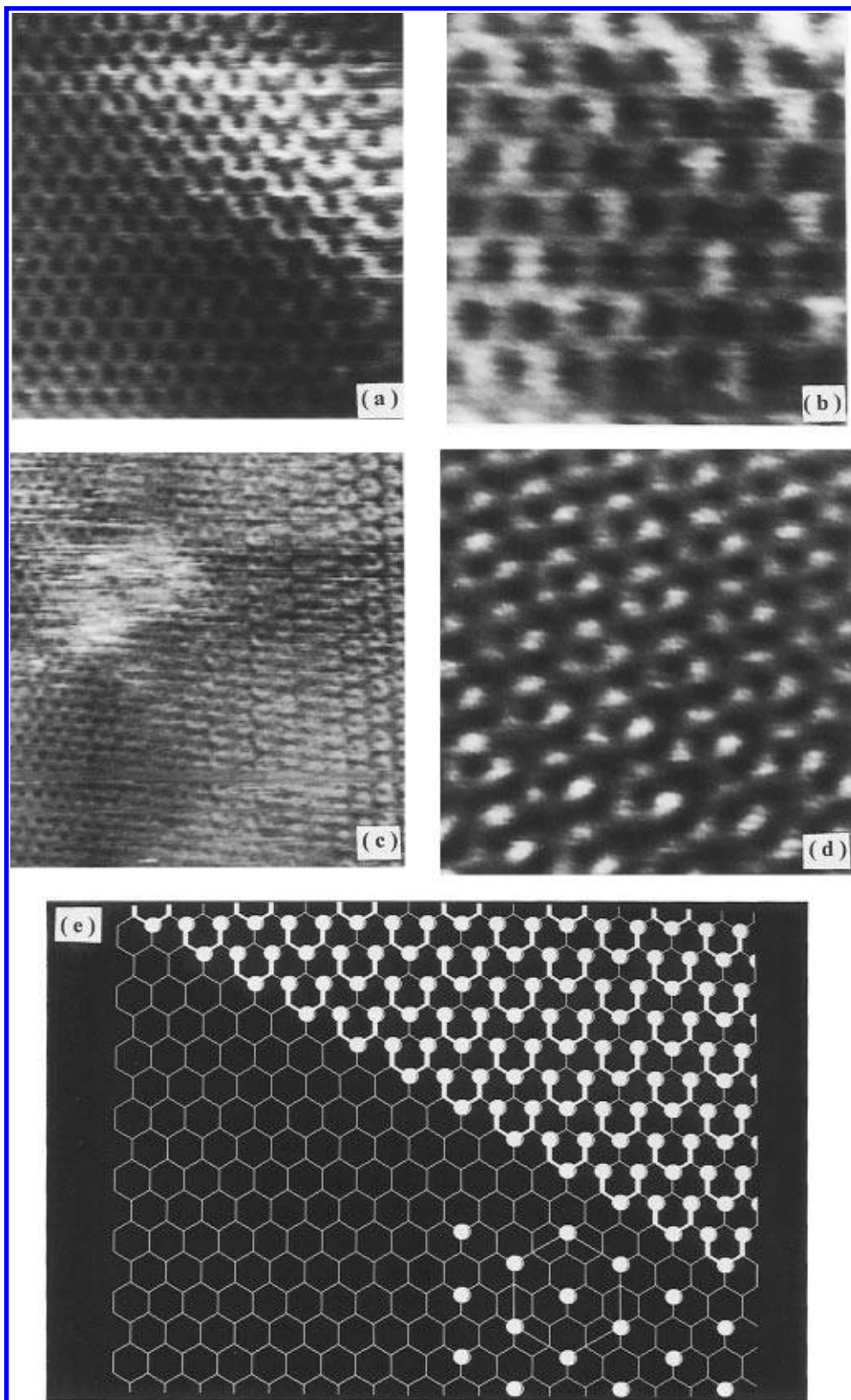(22) Gerischer, H. *Z. Electrochem.* **1950**, *54*, 540.

Figure 4. STM images (V_t = 2 mV; i_t = 1 nA) of HOPG after sulfur electrodeposition at the potential of peak A_1: (a) 4.0 × 4.0 nm^2 top view; (b) 1.7 × 1.7 nm^2 top view; (c) 6.0 × 6.0 nm^2 top view; (d) 1.9 × 1.9 nm^2 top view; (e) schemes of the ($\sqrt{3}\times\sqrt{3}$) and trimer structures showed in Figure 4. White circles indicate the position of S atoms. The underlaying HOPG honeycomb lattice is also shown.

surface[18] which occurs at potentials more positive than those corresponding to peaks A_1 and A_2. Thus, as in the working solution the HS$^-$ becomes the only significant species;[9] peak A_1 can be assigned to the electrooxidation of HS$^-$ ions yielding adsorbed sulfur species, which are electrodesorbed at peak C_1. On the other hand, peak A_2 can be attributed to the electrooxidation of HS$^-$ ions leading to elemental sulfur or polysulfide species. These species can be backwardly electroreduced to HS$^-$ ions in the potential range of peak C_2.[9-11,20] It should be noted

that the standard potential, E_r° for the reaction

$$SH^- + OH^- = S + H_2O + 2e^- \qquad (1)$$
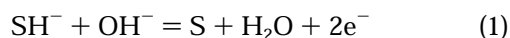
is $E_r^\circ = -0.226$ V.[23] In 10^{-3} M Na_2S borate–boric acid buffer (pH 8), the reversible potential of reaction 1 is $E_r \cong -0.43$ V at 298 K. Thus, peak A_1 at -0.80 V can be assigned to the formation of an initial adsorbed sulfur layer at about 0.4 V more negative than E_r, as has already been observed for different metals.[9] Considering S and C atomic radii, a close packed sulfur ML on HOPG would require $q_{ml} \cong 0.24$ mC cm^{-2}. Therefore, θ, the average S atom coverage, is given by the q_d/q_{ml} ratio. Accordingly, the θ vs t_d plot resulting from $E_d = -0.65$ V (peak A_1) reaches the limiting value $\theta \cong {}^1/_3$ ML for $t_d > 10$ s (Figure 1c). It should be noted that for sulfur deposited on metals in this potential range average values of θ are smaller than 0.4 ML.[24] On the other hand, the θ vs t_d plot resulting from $E = 0$ V (peak A_2) shows a continuous increase in the θ value to reach $\theta = 4$ ML for $t = 180$ s (Figure 1c). In this potential range linear θ vs $t_d^{1/2}$ plots have been obtained indicating that the multilayer growth behaves as a diffusion controlled process.

The second voltammetric scan recorded in the potential range of peaks A_1/C_1 (Figure 1d) shows a remarkable voltammetric charge decrease as compared to that observed in the first voltammogram. This means that the sulfur submonolayer remains bound to HOPG so that its complete removal from the substrate does not occur even by potential sweeping in the HER region. This explains why the charge of peak A_1 is greater than that of peak C_1 (Figure 1a). It should be noted that in this case peak C_1 is not clearly resolved even in the first voltammetric scan.

The height of peak A_1 increases linearly with v in the 0.01 V/s $< v <$ 0.3 V/s range (Figure 1e). This result confirms that the redox processes involving sulfide/sulfur species in the potential range of peak A_1 can be described as electrochemical surface reactions.

3.2. XPS Data. In order to confirm the nature of the electrooxidation compounds formed in the potential range studied in this work, XPS data were obtained after HOPG anodization at $E_d = 0.15$ V (peak A_2) for $t_d = 10$ s. For these electrodes XPS data show a large signal at 284.2 eV which corresponds to the 1s signal of C in graphite. In addition, a small peak can be observed at 163.5 eV, an energy value slightly smaller than those corresponding to 2p signals of S_8 (163.8 eV) and S_n (164.02 eV).[25] Although the peak energy is close to that of sulfur in elemental form, the presence of a small amount of polysulfide species cannot be unambiguously discarded.

3.3. STM Imaging. 3.3.1. Ex situ STM Imaging of HOPG Surfaces after Polarization at $E = -0.65$ V and $E = 0.15$ V in the Borate Buffer without Na_2S. It is well-known that STM imaging of HOPG surfaces may result in artifacts due to tip–surface interactions,[26] particularly when atomic resolution images are obtained using exceptionally low gap resistances (1 MΩ), such as multiple tip imaging leading to Moire patterns[27,28] and surface contamination.[29]

(23) *Standard Potentials in Aqueous Solutions*; Bard, A. J., Parsons, R., Jordan, J., Eds.; Marcel Dekker: New York, 1985.
(24) Halminton, I. C.; Woods, R. *J. Appl. Electrochem.* **1983**, *13*, 783.
(25) *Handbook of X-ray Photoelectron Spectroscopy*; Wagner, C. D., Riggs, W. M., Davis, L. E., Moulder, J. F., Muilenberg, G. E., Eds.; Perkin-Elmer Corporation: Eden Prairie, MN, 1978.
(26) Soler, J. M.; Baró, A. M.; Garcia, N.; Rohrer, H. *Phys. Rev. Lett.* **1986**, *57*, 444.
(27) Mizes, H. A.; Foster, J. S. *Science* **1989**, *244*, 559.
(28) Rousset, S.; Gauthier, S.; Siboulet, O.; Sacks, W.; Belin, M.; Klein, J. *Phys. Rev. Lett.* **1989**, *63*, 1265.
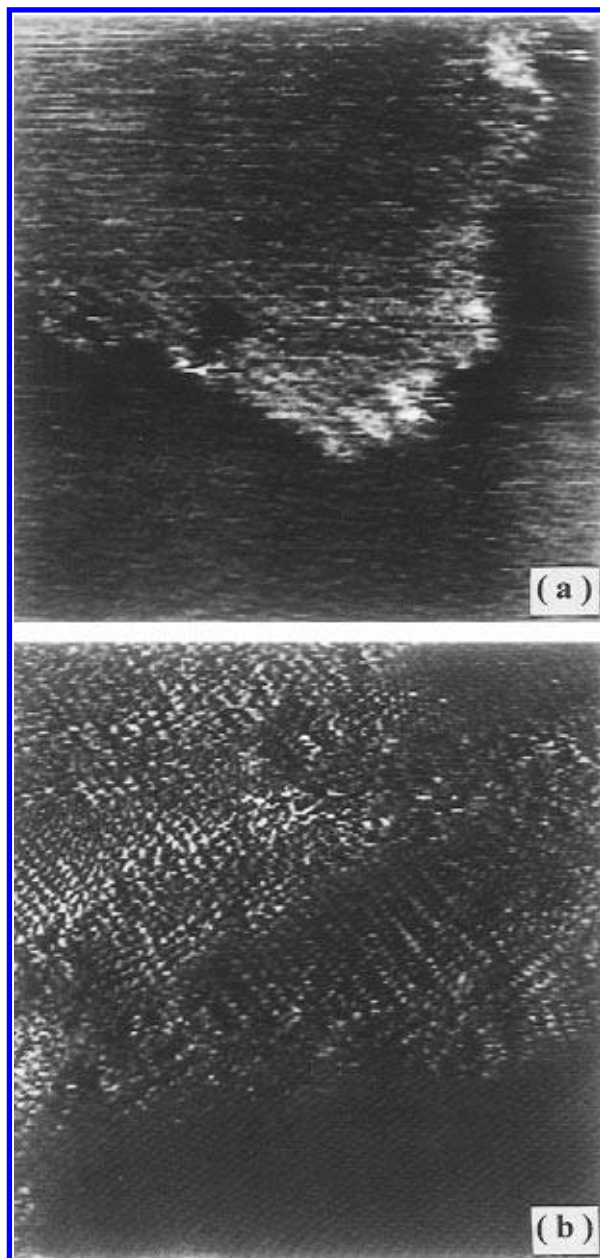(29) Rabe, J. P.; Sano, M.; Batchelder, D.; Kalatchev, A. A. *J. Microsc.* **1988**, *152*, 573.

Figure 5. Top view STM images of HOPG after sulfur electrodeposition at the potential of peak A_2: (a) 12×12 nm^2 topographic STM image ($V_t = 60$ mV; $i_t = 1$ nA); (b) 15×15 nm^2 constant height STM image ($V_t = 2.1$ mV; $i_t = 2$ nA).

In order to discard the possibility of any of these artifacts, control experiments were performed on HOPG electrodes held at $E = -0.65$ V and $E = 0.15$ V for $t = 10$ s in the borate buffer without Na_2S. A systematic imaging of these surfaces at high resolution and different tunneling conditions yielded either the low-resolution hexagonal lattice with $d = 0.24$ nm or the high resolution honeycomb lattice with $d = 0.14$ nm[19] even at bias voltages, V_t, as low as 1 mV and tunneling current, i_t, in the 1–5 nA range (Figure 2). As the honeycomb lattice was imaged with different tips, it is difficult to assign this structure to the presence of a multiple tip effect. In addition, the i_t vs V_t plots (Figure 3a) recorded at constant current at different fixed points of the surface are the same as those reported for HOPG.[30] Finally, after atomic resolution on sulfur domains, the HOPG atomic structure was repeatedly obtained at free sulfur domains of the electrode showing

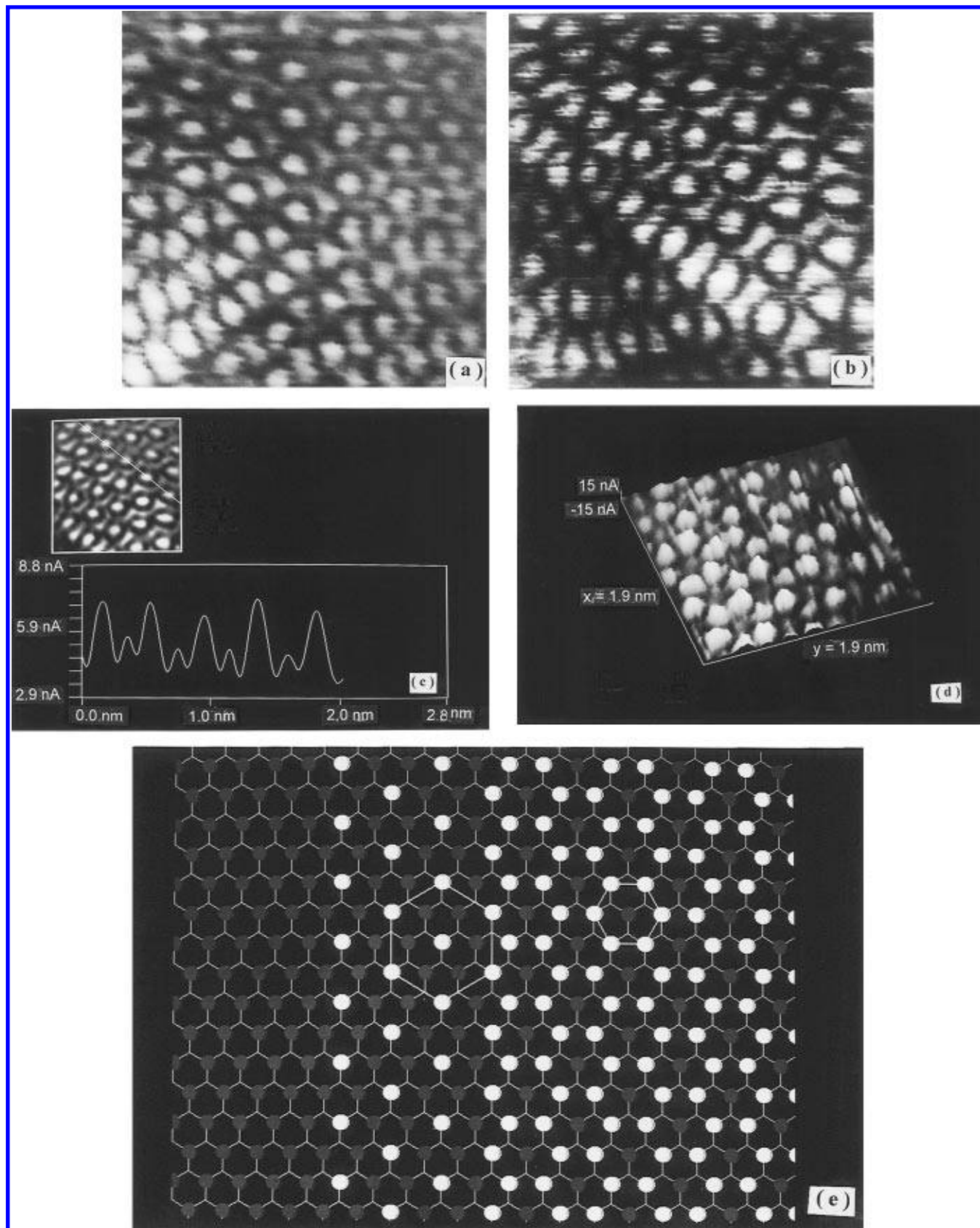(30) Watson, B. A.; Barteau, M. A.; Haggerty, L.; Lenhoff, A. M. *Langmuir* **1992**, *8*, 1145.

Figure 6. STM images of HOPG after sulfur electrodeposition at the potential of peak A_2: (a) 2.6×2.6 nm^2, top view; (b) 2.7×2.7 nm^2 top view. (c) Cross-section of STM image shown in Figure 6b; (d) 1.9×1.9 nm^2 (3D); (e) scheme of the $(\sqrt{3} \times \sqrt{3})R30°$ and honeycomb structures shown in Figure 6. White and dark dots indicate the position of S atoms on the second and first S atom layer, respectively.

atomic resolution images free of multiple tip effects. Thus, the presence of artifacts due to surface contamination and tip artifacts can be disregarded.

3.3.2. Ex Situ STM Imaging of Sulfur Electrodeposited at $E_d = -0.65$ V on HOPG. Sulfur deposits were grown at $E_d = -0.65$ V for $t_d = 10$ s for ex situ STM
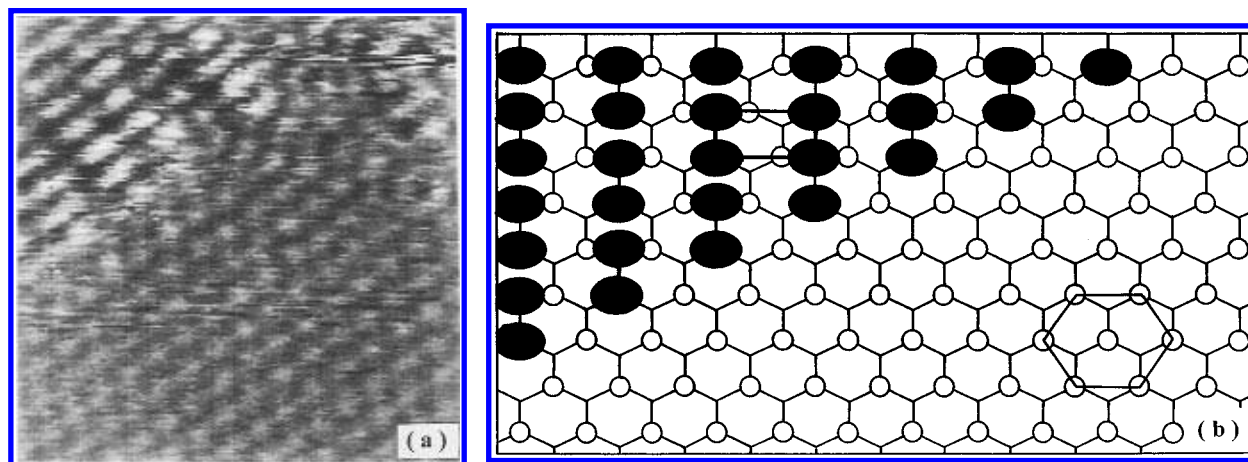
Figure 7. STM images of HOPG after sulfur electrodeposition at the potential of peak A_2 ($V_t = 2.1$ mV; $i_t = 2$ nA): (a) 3.0×3.0 nm^2 STM image top view; (b) scheme of the $[(1/2)\sqrt{3} \times (3/2)\sqrt{3}]$ rectangular sulfur structure shown in Figure 7a. Black dots indicate the position of S atoms on the second S atom layer whereas white dots indicate the underlaying filled hexagonal lattice.

imaging. The potential values for sulfur deposition are indicated by arrows in Figure 1b.

The atomic resolution STM image (Figure 4a) of HOPG with an average coverage by sulfur at $E_d = -0.65$ V, $\theta = 1/5$ ML, shows three different surface structures. One of these structures (Figure 4a, left-hand side) is the honeycomb lattice with $d = 0.14 \pm 0.01$ nm which corresponds to high-resolution STM images of HOPG.[19] Another structure can also be distinguished in Figure 4a (right-hand side, lower part) as a filled hexagonal pattern. The presence of this structure is much better disclosed by zooming (Figure 4b) a small area of the STM image shown in Figure 4a. The elongated spots in Figure 4b, which are placed atop C atoms with one spot for each graphite hexagon, lead to a ($\sqrt{3} \times \sqrt{3}$) filled hexagonal array with $d = 0.42 \pm 0.02$ nm. According to experimental data,[2-4] S atoms should appear as protrusions when they are imaged on metals at low bias voltages and low tunneling currents. Thus, in principle, the elongated spots shown in Figure 4b can be assigned to a diluted sulfur submonolayer on HOPG. The S atom surface coverage at this submonolayer is $\theta_s = 1/6$ ML. A third type of structure appears in Figure 4a (right-hand side, upper part) as bright ring patterns displaying a hexagonal array. This pattern can be assigned to sulfur rings formed on C hexagons, the distance between ring centers being $d = 0.42 \pm 0.02$ nm. A more detailed image of these rings resembling closely those reported for sulfur on Re (see Figures 4 and 6 in ref 3) is shown in Figure 4c. In some images the ring structure is resolved (Figure 4d). These images reveal that rings are formed mainly by sulfur trimers placed on C hexagons with S atoms at $d(S-S) = 0.24 \pm 0.02$ nm rather than at $d(S-S)$ expected from sulfur.[31] Similar trimers formed by S adatom clustering were also observed for S on Re-(0001) in UHV conditions[3,4] indicating that it is a characteristic structure of sulfur deposition at the monolayer level. In this case it has been found that the $d(S-S)$ in trimers corresponds to the $d(Re-Re)$ and not to that expected from sulfur. As trimers grow together they create the impression of a hexagonal lattice with $d = 0.24$ nm as seen in Figure 4d (right-hand side).

Although the interpretation of STM images in terms of geometry, especially on HOPG, should be made with great caution, the fact that both the substrate lattice and adsorbed atoms are simultaneously imaged allowed us to propose a plausible model for the S adsorption on HOPG (Figure 4e). Thus, at the low right hand side of Figure

4e, diluted S atom adsorbate structures are shown, whereas the upper right hand side pattern displays a S trimer network atop the HOPG lattice. It should be noted that this model implies S atoms located on top of C atoms as seen in the STM images. On the contrary, for transition metals experimental data indicate that S atoms adsorb at hollow sites.[4] Theoretical calculations of S atom adsorption on transition metals[32] suggested that S atoms in hollow sites would produce maxima in constrast to S atoms on top sites. On the other hand, adsorption of different gases also occurs at hollow sites of the HOPG lattice. Accordingly, it appears that S adsorption on top of C atoms is unlikely. However, theoretical calculations employing a semiempirical Hamiltonian[33] for S adsorption on HOPG for top, bridge, and hollow positions indicate that the formation of a S−C bond is largely favored for both on-top and bridge positions. Moreover, calculations for three S atoms on HOPG clusters also show that a trimer structure with $d(S-S) = 0.24$ nm on top of C atoms as proposed in Figure 4e is energetically favored.

Occasionally, tetramers 0.24×0.15 nm^2 in size were also imaged. It appears that tetramers are formed by at least two C atoms. The value $d = 0.15$ nm is close to $d(C-C)$ in HOPG and much smaller than $d(S-S) \cong 0.2$ nm. At present, we are unable to advance an unambiguous identification of other atoms in the tetramer structure.

Finally, it should be noted that the STM images always show bare HOPG and sulfur submonolayer domains. The values of θ_s for these submonolayer domains are between $1/6$ and $1/2$ ML. Then, taking into account the presence of bare HOPG regions, these figures are consistent with $\theta = 1/5$ ML derived from electrochemical data.

3.3.3. Ex Situ STM Imaging of Sulfur Electrodeposited at $E_d = 0.15$ V on HOPG. The ex situ STM images of sulfur electrodeposits produced at $E_d = 0.15$ V, comprising a charge density equivalent to 2 ML ($q_d = 0.5$ mC cm^{-2}), obtained in the topographic and in the constant height modes (Figure 5) also show discontinuous sulfur deposits consisting of covered and bare HOPG regions. Some regions exhibit those ring structures already described for the sulfur deposits grown at $E_d < E_r$, as well as rows of elongated elements leading to rectangular arrays and hexagonal patterns. STM images containing adjoining patches involving the substrate lattice and the sulfur adlattice were also obtained for overpotential deposited sulfur on Au(111).[12]

(31) Dounthy, J. C.; Ogletree, D. F.; Salmeron, M. C.; Sautet, P.; Bouquet, M. L.; Joachim, C. *Ultramicroscopy* **1992**, *42-44*, 490.
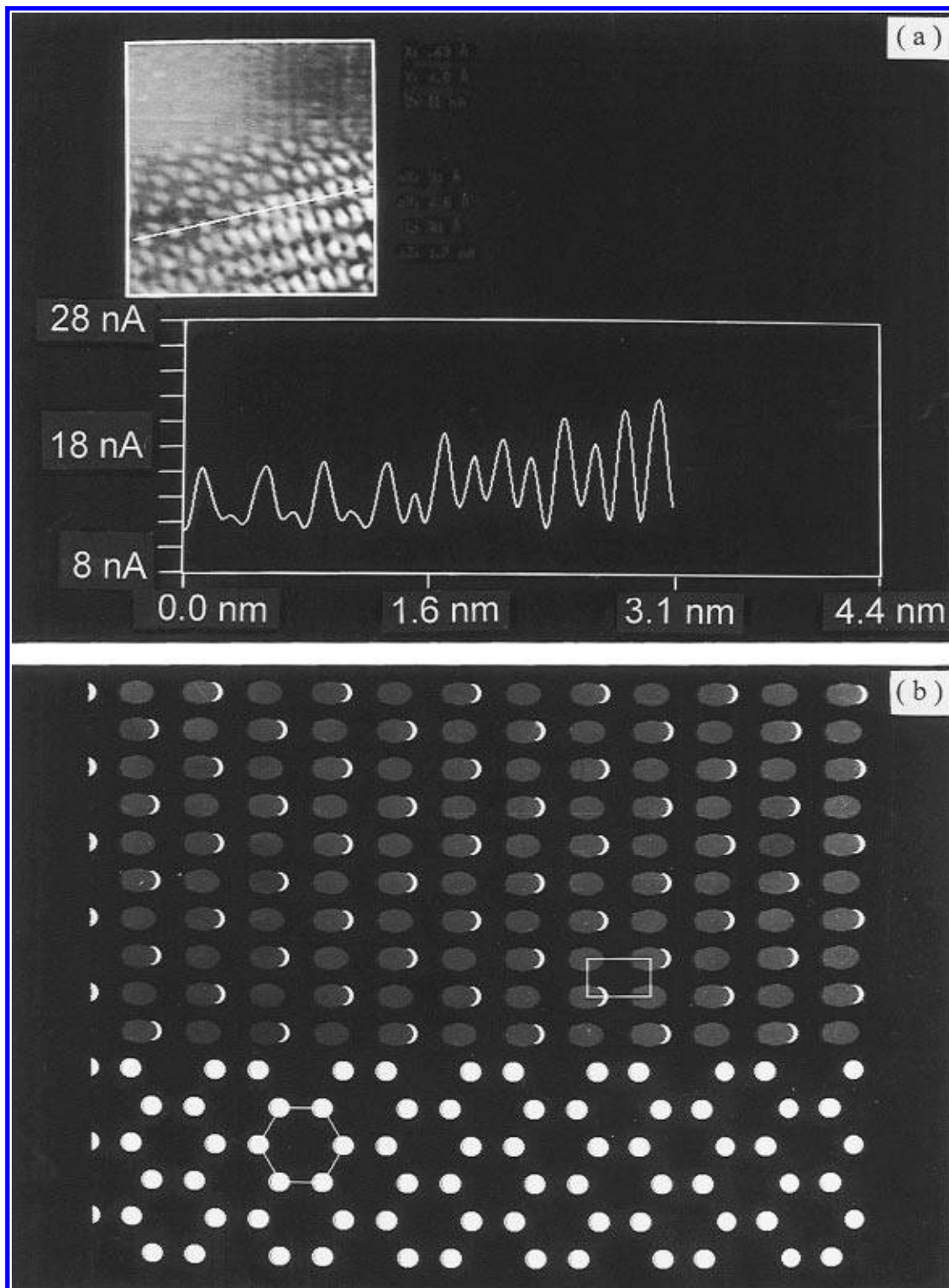
(32) Mayer, B. *Chem. Rev.* **1976**, *76*, 367.

(33) Mola, E. E.; Vicente, J. L.; Appignanesi, G.; Zubimendi, J. L.; Salvarezza, R. C.; Arvia, A. J. Submitted for publication.

Figure 8. STM images of HOPG after sulfur electrodeposition at the potential of peak A_2: (a) 2.9×2.9 nm^2 STM image top view and cross section; (b) scheme for the rectangular sulfur structure. Dark and white dots indicate the position of S atoms at the third and second S atom (honeycomb) layer, respectively.

Transition regions from sulfur submonolayer domains in contact with the HOPG to other more complex sulfur patterns on HOPG were also imaged. Thus, the transition from the trimer structure, which corresponds to sulfur submonolayer domains in the first layer (Figure 6a, right-hand side, lower part), to a filled hexagon pattern with $d = 0.42 \pm 0.02$ nm (Figure 6a, upper part) can be observed. Furthermore, the transition from the filled hexagonal patterns structure to a dense honeycomb pattern with $d = 0.24 \pm 0.02$ nm (Figure 6a, left-hand side) can also be clearly seen.

The ball-like features in the filled hexagon pattern with $d = 0.42 \pm 0.02$ nm (Figure 6b, raw data) form a $(\sqrt{3} \times \sqrt{3})$-$R30°$ lattice ($\theta_s = 1/3$ ML) atop the underlying trimer lattice. Thus, the cross section (Figure 6c) of Figure 6b shows sulfur atoms in trimers as small protrusions in between ball-like features. These features can be, in principle, assigned to S atoms placed atop S atoms forming trimers in contact with HOPG.

Another structure consisting of a honeycomb pattern with $d = 0.24 \pm 0.02$ nm was imaged simultaneously with the $(\sqrt{3} \times \sqrt{3})R30°$ lattice and the underlying trimer lattice

(Figure 6d). Seemingly, the honeycomb lattice is related to a more dense array of S atoms consisting of two S atoms on each trimer of the first layer leading to $\theta_s = {}^2/_3$ ML.

It should be noted that $(\sqrt{3} \times \sqrt{3})R30°$ ($d = 0.42$ nm) and honeycomb ($d = 0.24$ nm) superstructures have been imaged on HOPG near absorbates, and near defects,[27,29,34] and also after HOPG exposure to low-energy-ion impacts.[34] These superstructures on HOPG were electronic in nature rather than assignable to a HOPG lattice reconstruction. However, it seems unlikely that this explanation could be extended to the STM images shown in Figure 6a,d because these superstructures lie atop the trimer structure which certainly cannot be assigned to HOPG. It appears that the $(\sqrt{3} \times \sqrt{3})R30°$ ($d = 0.42$ nm) and the honeycomb ($d = 0.24$ nm) superstructures could be related to the second sulfur layer built up on sulfur submonolayer domains in contact with HOPG. A tentative model accounting for the second layer sulfur atoms is depicted in Figure 6e. This scheme displays the lattice of two types of S hexagons.

However, the predominant structure observed for overpotential deposited sulfur on HOPG (Figure 5) consists of parallel rows made of large elongated balls with $d = 0.21 \pm 0.02$ nm, and a distance between nearest neighbor parallel rows $d = 0.37 \pm 0.02$ nm (Figure 7a). Accordingly, elongated balls form a $[(1/2)\sqrt{} \times (3/2)\sqrt{3}]$ rectangular lattice with one edge following the $\sqrt{3}$-direction and another edge following the directions of underlaying filled hexagonal lattice. This surface structure resembles the rectangular arrays of elongated balls found for sulfur/Re(0001) system in UHV[4] which have been assigned to S atoms. Therefore, the elongated balls in the rectangular patterns (Figures 5b and 7a) can also be assigned to S-atoms in islands with a second S layer.

The rectangular lattice can also be originated from the $(\sqrt{3} \times \sqrt{3})R30°$ ($\theta_s = {}^1/_3$) structure simply by adding a S atom between two S atoms in the underlaying trimer lattice, as schematically shown in Figure 7b. This procedure leads to rows of S atoms with $d(S-S) = 0.21$ nm, i.e. the S−S distance in bulk sulfur, with the parallel rows separated by $d(S-S) = 0.37$ nm ($\theta_s = {}^2/_3$).

The analysis of the STM image shown in Figure 8a reveals that the rectangular patterns with 0.21 nm $\times$ 0.37 nm are also associated with a third sulfur layer on sulfur islands. In this image a honeycomb structure with $d = 0.24$ nm together with rows of elongated balls is observed. The cross section of this image shows that elongated balls are placed atop the honeycomb structure. Then, it is reasonable to conclude that these rectangular patterns involve a third S atom layer atop the second sulfur layer as schematically shown in Figure 8b.

3.3.4. STM Imaging Conditions for Sulfur-Covered Domains. High-quality STM images of sulfur-covered domains were systematically obtained in the 1 mV $< V_t <$ 5 mV and 1 nA $< i_t <$ 5 nA range (gap resistance around 1 MΩ) in the constant height mode. Thus, tip−graphite interactions leading to artifacts could appear during the imaging process. It should be stressed that gap resistances as low as 20 MΩ have been employed to obtain atomic resolution images of sulfur on Re(0001) in an UHV environment without tip or surface damage.[3] However, in our case, we were able to image the adsorbate structures at gap resistances as high as 100 MΩ, although with a certain deterioration of the image quality (Figure 9). Thus, we can conclude that these structures are not artifacts originated by the low gap resistance conditions. However, it should be stressed that at 1 MΩ strong forces
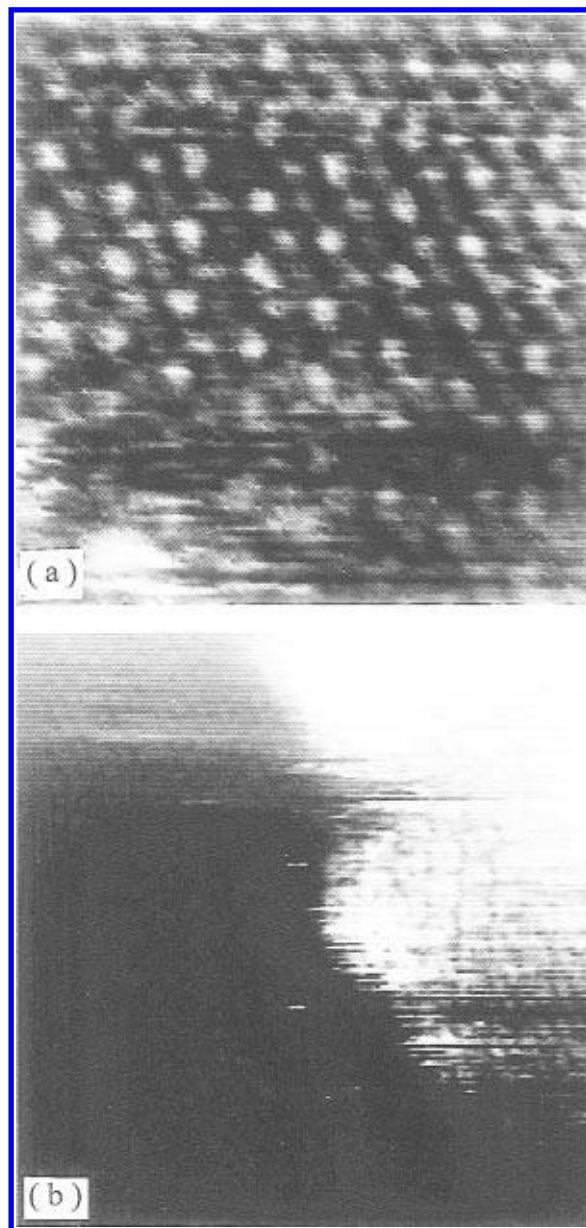
(34) Albrecht, T. R.; Mizes, H. A.; Nogami, J.; Sang-il Park; Quate, C. F. *Appl. Phys. Lett.* **1988**, *52*, 362.

(35) Shedd, G. M.; Russell, P. E. *J. Vac. Sci. Technol.*, A **1991**, *9*, 1261.

Figure 9. Top view STM images ($V_t = 60$ mV; $i_t = 2$ nA) of HOPG after sulfur electrodeposition at the potential of peak A_2: (a) 2.8×2.8 nm^2 STM image showing the $(\sqrt{3} \times \sqrt{3})R30°$ and honeycomb sulfur structures; (b) 6.0×6.0 nm^2 STM image displaying sulfur rings (right) coexisting with the HOPG hexagonal filled structure (top left).

are clearly present between tip and surface. Thus, the fact that S atoms are not displaced or scrapped from the HOPG surface suggests the S−HOPG interaction is larger than that obtained from simple physisorption. In fact, S atoms adsorbed at peak A_1 remain on the HOPG surface even after cathodization in the HER region for several minutes. Accordingly, the adsorption energy of S atoms on top sites and bridge sites derived from quantum chemistry calculations is in the $0.3-0.4$ eV[33] range.

Topographical imaging of sulfur deposits was routinely obtained (Figure 5a). However, the quality of atomic resolution at sulfur domains in these STM images was lower than that obtained in the constant height STM imaging mode. Although the I_t vs V_t curves on HOPG and most semiconductors are "nonspecific", the I_t vs V_t plots recorded on sulfur-covered domains differ from that obtained on the HOPG domains (Figure 3). In all cases the I_t vs V_t plots at sulfur domains exhibit a marked increase in current at both negative and positive V_t as

compared to those recorded on HOPG. Preliminary results from semiempirical calculations suggest that S adsorption on HOPG increases the density of states at the Fermi level.[33]

The fact that many sulfur structures have hexagonal symmetry with d(S−S) close to substrate atom distances is not surprising as it is well-known that adsorbates at the monolayer level, particularly sulfur, follow the substrate periodicity,[3,4] i.e. $(\sqrt{3}\times\sqrt{3})R30°$ structures on the (111) and (0001) surfaces of fcc and hcp metals.[1,6,7] Moreover, the imaging of a rectangular structure is consistent with the other structures observed, and it further contributes to disregard any influence of the tip−graphite interactions on the STM images.

4. Conclusions

(i) Atomic resolution ex situ STM images of sulfur deposited at potentials either more negative or more positive than E_r on HOPG from a Na_2S-containing borate−boric acid buffer (pH 8) show in both cases the formation of discontinuous deposits (islands) with different surface structures. These surface structures cover from sulfur submonolayer domains to three sulfur layer islands.

(ii) Ex situ STM images of HOPG electrodes held at potentials more negatives than E_r in Na_2S-containing solutions show uncovered regions and sulfur submonolayers with $\theta_s = 1/6$ ML and $\theta_s = 1/2$ ML. These figures are consistent with the average $\theta = 1/3$ ML derived from electrochemical measurements.

(iii) For sulfur deposits made at potentials more negative than E_r, results are either d(S−S) = 0.42 ± 0.02 nm or d(S−S) = 0.24 ± 0.02 nm, depending on the θ_s value. The sulfur submonolayer structures follow either the HOPG or the $\sqrt{3}$-direction. These d(S−S) values are greater than the d(S−S) value in elemental S. These results indicate a strong interaction between the electrodeposited S atoms and the HOPG substrate.

(iv) The formation of sulfur trimers should also be mediated by the substrate as d(S−S) $\cong$ 0.24 nm exceeds that corresponding to bulk S. In trimer formation, S−S atom and the trimer−substrate interactions determine the overlayer structure.

(v) Ex situ STM images of overpotential deposited sulfur show submonolayer domains as well as surface structures similar to those imaged for sulfur deposits grown at $E_d <$ E_r and others corresponding to the second and the third sulfur layer at islands.

(vi) The second sulfur layer surface coverage ranges from $\theta_s = 1/3$ ML in the $(\sqrt{3}\times\sqrt{3})R30°$ lattice with d(S−S) = 0.42 ± 0.02 nm, to $\theta_s = 2/3$ ML in both the honeycomb and the rectangular lattice. For these structures ($\theta_s = 2/3$ ML) the position of the S atom added to the $(\sqrt{3}\times\sqrt{3})R30°$ lattice determines an interatomic distance greater than (honeycomb lattice, d(S−S) = 0.24 ± 0.02 nm) or equal to (rectangular lattice, d(S−S) = 0.21 ± 0.02 nm) d(S−S) in bulk sulfur.

(vii) The S atom rows with d(S−S) = 0.21 nm in the rectangular arrays observed for the second and third sulfur layer at islands are consistent with the appearance of the elemental sulfur XPS signal at overpotential deposited S/HOPG specimens.